Planetary Shock Waves

WILLIAM K. DEWAR

Department of Oceanography and Supercomputer Computations Research Institute, Florida State University, Tallahassee, FL 32306

(Manuscript received 27 May 1986, in final form 26 September 1986)

ABSTRACT

A number of general circulation models have recently been proposed that compute the steady-state structure of the general circulation. Observations of 18°C water formation, on the other hand, suggest the need for a study of the time-dependent large-scale structure of the oceans. In this paper, the planetary geostrophic equations are used to compute the evolution of large-scale thermal anomalies with a view toward understanding the variability in the general circulation caused by water mass formation events.

The evolution of a thermal anomaly is considered in the absence of wind forcing. In this case, the planetary geostrophic equations can be reduced to a first-order equation, the Planetary Geostrophic Wave Equation (PGWE). Arbitrary initial conditions governed by the PGWE tend to steepen and, under an assumed diffusive closure, form shock waves. The evolution of an initially columnar eddy is obtained, and four different phases of shock propagation are identified. The implications for heat transport, potential vorticity transport and thermocline ventilation are discussed.

1. Introduction

The structure of the oceanic permanent thermocline has been examined in a number of recent papers (Rhines and Young, 1982a,b; Young and Rhines, 1982; Luyten et al., 1983; Pedlosky and Young, 1983). Subsequent data analysis (McDowell et al., 1982; Keffer, 1985) has tended to confirm many of the predictions in these theories, suggesting that the models are illuminating with respect to ocean dynamics. The basic ideas behind all the recent thermocline theories are 1) that the net circulation transport is limited by the Sverdrup constraint and 2) that away from lateral and vertical boundaries the flow is very nearly conservative. Rhines and Young (1982a), however, point out that weak dissipation can have substantial effects in the proper circumstances.

A common feature of all these models is that they compute the steady state structure of the thermocline subject to imposed time-independent boundary conditions. It is well known, however, that the large-scale oceanic forcing functions are variable. Observational evidence continues to mount suggesting the existence of important time dependence in thermocline structure. For example, Talley and Raymer (1982) discuss variability in the properties of 18°C water, the subtropical mode water of the North Atlantic. They point out that while the T–S properties of 18°C water are slow to change, the amounts of observed 18°C water, its potential vorticity and the thermocline structure about the 18°C sigma-theta surface are highly time dependent. They suggest that 18°C water is formed by late winter overturning in the northern part of the subtropical gyre, and that advection by the Sverdrup flow transports the 18°C "plugs" about the basin. Talley and Raymer use data from the Panulirus station (located in the general westward return flow of the North Atlantic) to support these points by noting that the arrival times of 18°C water (characterized by the joint occurrence of a finite amplitude event in the $\sigma_\theta = 26.5$ surface and a minimum in potential vorticity) were suggestive of late winter formation, and that during certain several year periods no evidence for 18°C water production could be found.

Although the dynamical role of subtropical mode water is not yet clear, recent theoretical studies (Dewar, 1986; Cushman-Roisin, 1987) suggest strongly that it is a feature of substantial importance to the wind-driven gyre structure. There is thus a need for time-dependent theories of the large-scale circulation to clarify the dynamics of 18°C water formation events, to indicate what effects these events have on the time-averaged fields, and to complement those steady state theories that have proven to be so useful. In the present paper, some simple models of the time-dependent response of the large-scale are examined with a view toward understanding 18°C water evolution.

Prior studies of the time-dependent response of the large scale have considered the evolution of an initially resting ocean, subject to an impulsively applied wind stress. Anderson and Gill (1975) pointed out that the ocean responds in this case by emitting a long, nondispersive baroclinic Rossby wave from the eastern ocean boundary and that the Sverdrup balance is established in its wake. Similar results in an ocean with weak bottom topography were found by Anderson and Killworth (1977). In a later paper, Anderson and Killworth (1979) considered the effects of finite amplitude

on the propagation of large-scale thermocline waves and applied the results of that analysis to the spinup problem. They found that the westward propagation of the emitted baroclinic wave was accelerated from that of the quasi-geostrophic wave, and that the rear face of the wave tended to steepen. Both of these results were confirmed by numerical experimentation with a reduced gravity, shallow water model. Johnson and Willmott (1981) noted similar results in their numerical model, and Willmott (1985) suggested that steepening and breaking might account for the lack Rossby wave activity in the North Pacific. A basic result of these studies is that the large-scale adjustment to variability in forcing occurs in the time necessary for a baroclinic wave to transit the basin.

A fully nonlinear, quasi-geostrophic spinup problem was considered by Dewar et al. (1984). This study differed from previous work in that the baroclinic Rossby wave propagated in the presence of the Sverdrup transport. The steady Rhines and Young (1982b) theories predicted the existence of closed circulation regions, inside of which dissipation was important. Dewar et al. (1984) demonstrated that inside these closed regions, spinup involved the shear dispersion of potential vorticity and that a so-called averaging time was necessary to bring about a steady state. Eddy resolving spinup calculations demonstrate essentially the same behavior.

The present study differs from previous studies in that 1) the variability is assumed to occur in the buoyancy forcing (rather than in the wind forcing), 2) no quasi-geostrophic approximations are made, and 3) two active layers are included. The system is weakly nonconservative and the thermocline anomalies are assumed to be finite in amplitude.

This paper is organized as follows. The model and the governing equations are introduced in section 2. After some algebra, the system is reduced to one equation in one unknown, including explicit time dependence, buoyant forcing and wind forcing. This equation is further reduced to a simple wave equation by choosing special forms for the forcing functions. The characteristics of this wave equation and some of its solutions are discussed in section 3. It is shown that the governing equation leads to a steepening of arbitrary initial conditions. A simple parameterization of eddy effects is then employed that both combats the steepening and leads to the formation of shock waves. A detailed solution of the system subject to an initial condition representing a "plug" of newly formed 18°C water is obtained. Accordingly, the solution breaks neatly into four phases, divided in time by the propagation tendencies of the shock waves. The results of the analysis are reviewed and comparisons with data are presented in the discussion section.

2. Model development

Consider the system in Fig. 1. The ocean will be modeled as a rotating two-layer fluid with a flat bottom.

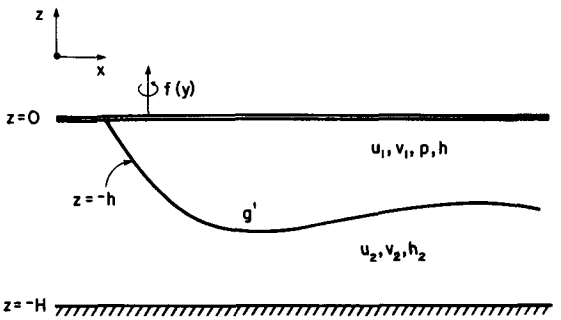

FIG. 1. Two-layer system. Variables in the upper layer are denoted with the subscript 1, those in the lower layer with the subscript 2. The upper layer has a thickness h, and the total fluid depth is H. The Coriolis parameter, f, is a function of latitude. A rigid lid is applied and the bottom is assumed to be flat.

Upper layer quantities will be denoted by the subscript 1 and lower layer quantities by the subscript 2; accordingly, the upper layer dynamic pressure is P_1 and the lower layer dynamic pressure is P_2. The Coriolis parameter is f, and its north–south gradient is β. The total fluid depth will be denoted as H and the upper layer thickness as h. The quantities u_i and v_i are east and north velocities, respectively.

a. Equations of motion

The starting point for this analysis will be the planetary geostrophic equations. These can be obtained asymptotically from the full equations of motion if the Rossby number is small and the motion is planetary in scale (Pedlosky, 1979). Furthermore, it is assumed that the fluid is Boussinesq. The dynamical equations in each layer are thus geostrophy and heat conservation:

$$fu_i = -\frac{\partial}{\partial y}P_i + \left[\frac{\partial}{\partial z}\tau_{(y)}\right] \tag{1a}$$

$$fv_i = \frac{\partial}{\partial x}P_i - \left[\frac{\partial}{\partial z}\tau_{(x)}\right] \tag{1b}$$

$$(h_i)_t + \left(\int^{h_i} u_i dz\right)_x + \left(\int^{h_i} v_i dz\right)_y = (-1)^i S \tag{1c}$$

where (x, y, z) are Cartesian coordinates in the east, north and vertical directions. Here $h_1 = h$, $h_2 = H - h$, and the vertical integrals are taken over the ith layer. Frictional momentum transfers are denoted in the horizontal momentum equations by the normalized turbulent stress vector $\boldsymbol{\tau} = (\tau_{(x)}, \tau_{(y)})$, where $\boldsymbol{\tau}$ is stress divided by a reference density. The quantity S is a buoyantly driven cross-interfacial flow, and $S \sim F/g'$ where F is the surface buoyancy flux from the ocean to the atmosphere and g' is reduced gravity. Positive S denotes a heat loss from the ocean. A two-layer fluid accommodates this heat loss by converting warm water to cold, or equivalently by shrinking the upper layer ($h_t < 0$). A negative S value causes the upper layer to thicken in response to the addition of heat.

A rigid lid is applied at the ocean surface, which insures that the barotropic adjustment of the fluid is instantaneous. Wind stress and buoyancy flux boundary conditions are also applied at the surface. (Note: Salinity is neglected, so the fluid buoyancy is proportional to temperature.) Momentum flux, heat flux and vertical velocity will all be assumed to vanish at the ocean bottom.

b. Reduction to one equation in one unknown

Substituting with geostrophy for the velocities in the upper layer heat equation (1c) yields

$$h_t+\frac{1}{f}J(P_1,h)-\frac{\beta}{f^2}hP_{1x} = -\text{curl}\left(\frac{\tau_0}{f}\right)+\text{curl}\left(\frac{\tau(x,y,-h)}{f}\right)-S \quad (2)$$

where J denotes the usual Jacobian operator:

$$J(A,B)=A_xB_y-A_yB_x,$$

τ_0 denotes atmospheric stress, $\tau(x, y, -h)$ the frictional stress occurring at the interface and "curl" denotes the vertical component of the curl operator:

$$\text{curl}(A\hat{i}+B\hat{j})=B_x-A_y.$$

In Eq. (2) $\tau(x, y, -h)$ represents that fraction of the momentum forcing communicated to the lower layer. Only that part of the wind momentum remaining in the upper layer can drive an upper layer divergence.

Adding the heat equations (1c) yields

$$\left(\int_{-h}^{0}u_1dz+\int_{H}^{-h}u_2dz\right)_x+\left(\int_{-h}^{0}v_1dz+\int_{-H}^{-h}v_2dz\right)_y=0. \quad (3)$$

If u_i and v_i are eliminated from (3), a nonlinear form of the Sverdrup balance is obtained:

$$\frac{\beta}{f^2}[HP_{1x}+g'hh_x-g'Hh_x]=\text{curl}\left(\frac{\tau_0}{f}\right). \quad (4)$$

Equation (4) can be integrated westward from the eastern boundary x_e where the upper layer thickness and pressure are presumed to be known:

$$HP_1+\frac{g'h^2}{2}-g'Hh=\phi(x,y) \quad (5)$$

where

$$\phi(x,y)=\frac{f^2}{\beta}\left\{\int_{x_e}^{x}\text{curl}\left(\frac{\tau_0}{f}\right)dx\right\}+HP_1(x_e)+g'\frac{h^2(x_e)}{2}-g'Hh(x_e).$$

Equation (5) can then be used to eliminate P_1 from (2). The result is

$$h_t+\frac{1}{fH}J(\phi,h)-\frac{\beta}{f^2}\frac{h}{H}\phi_x-\frac{\beta h}{f^2H}(g'Hh_x-g'hh_x) = -\text{curl}\frac{(\tau_0-\tau(x,y,-h))}{f}-S+\text{other}. \quad (6)$$

Equation (6) is the planetary geostrophic thermocline equation. It relates changes in layer thickness to advection by the Sverdrup flow, planetary vortex stretching, β-driven westward propagation, wind-driven divergence and buoyancy forcing. Other effects, such as diffusion and smaller scale processes, are grouped in the term labeled "other." These are presumed to be small, for the most part, as required by the scaling.

One could specify wind and buoyancy forcing functions and solve (6) for the subsequent thermocline evolution. Indeed, this would address the primary objective of this paper, which is to consider the variability induced in the large-scale by time-dependent forcing. For the remainder of this paper, however, I will investigate a simplified form of the thermocline equation obtained by setting ϕ, τ_0, $\tau(x, y, -h)$ and S all to zero. The rationale for studying this limit will be given shortly. For now, it is sufficient to note that this corresponds to the adiabatic, inviscid, unforced limit of the thermocline equation. The resulting simplified equation,

$$h_t-\frac{\beta g'}{f^2}\left(hh_x-\frac{h^2h_x}{H}\right)=\text{other}, \quad (7)$$

will be called the Planetary Geostrophic Wave Equation (PGWE). It governs the finite amplitude evolution of thermal anomalies at planetary scales. Anderson and Killworth (1979) considered a form of the PGWE appropriate to a reduced gravity model. Their equation is obtained from (7) by letting H become large, which has the effect of dropping the dominant nonlinearity in the PGWE from cubic to quadratic.

A number of simplifications were employed in going from the thermocline equation to the PGWE. I would nonetheless like to argue that the PGWE is a viable model equation to apply to 18°C water. The reasons for this are best explained via a simple thought problem (see Fig. 2). Consider an initially warm layer that is subjected to a limited extraction of heat over a limited area. Because this is a two-layer fluid, a thermocline builds up from the bottom of the ocean, as indicated by the dashed lines in Fig. 2. Fast barotropic waves are emitted during this process, but if the heat is withdrawn quickly enough, the fluid is unable to respond baroclinically. Thus, the thermocline builds almost passively (balanced, of course, by a geostrophic flow) until the cooling is shut off.

This scenario is in ways crudely reminiscent of the creation of 18°C water. Cornillon (personal communication, 1986) suggests on the basis of satellite SST observations in the North Atlantic that 18°C water is formed for only a few weeks during the year, and then at preferred locations within the subtropical gyre. Once the convective overturning halts, however, a thin, in-

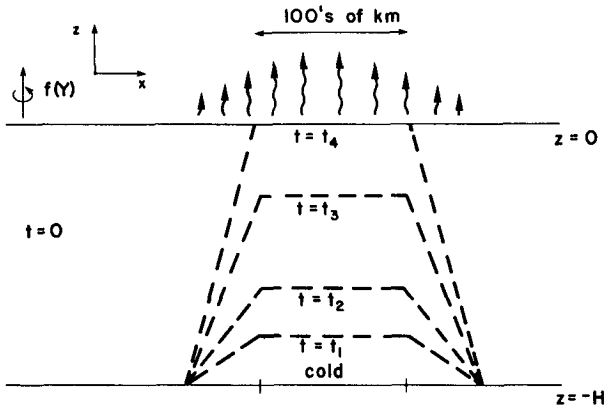

FIG. 2. Thermocline set-up. The ocean is assumed to be initially homogeneous and warm. Heat is subsequently extracted over a limited region, as indicated by the wavy arrows. If the heat is extracted rapidly enough, the fluid is unable to adjust baroclinically, and the thermocline builds upward from the bottom. Thermocline depths at later times are indicated by the dashed lines. Once the thermocline has broken the surface, the cooling is assumed to shut off.

sulating surface layer builds on top of the 18°C plug, and the diabatic modification of the subsurface waters stops. One can thus argue from the vantage point of baroclinic evolution that 18°C water formation is an instantaneous event, that all of the required buoyant flux to the atmosphere is associated with its formation, and that the baroclinic evolution of 18°C water proceeds in the absence of diabatic effects. This is the rationale for ignoring S in (6) and considering 18°C water evolution in the realm of initial value problems. The reason for ignoring wind forcing in (6) is to focus as much as possible on the dynamic evolution of the thermal anomaly.

3. Properties and solutions of the PGWE

Under the assumption that the right-hand side of (7) is small, the PGWE is roughly a nonlinear, first order partial differential equation and can be solved using the method of characteristics. Introducing s as the coordinate along the characteristics and r as the coordinate across the characteristics, (7) can be reduced to the coupled set of equations:

$$\frac{\partial}{\partial s}t = 1 \tag{8}$$

$$\frac{\partial}{\partial s}x = \frac{-\beta g'}{f^2}\left(h - \frac{h^2}{H}\right) = c(h) \tag{9}$$

$$\frac{\partial h}{\partial s} = 0 \tag{10}$$

with the initial conditions

$$s = 0, \quad h = h_0(r) \quad \text{at} \quad t = 0.$$

Note the definition of $c(h)$ in (9). The implicit solution of (8)–(10) is

$$h = h_0\left[x + \frac{\beta g'}{f^2}\left(h - \frac{h^2}{H}\right)t\right]. \tag{11}$$

Note that the dependence of the solution on y can be carried parametrically. Equation (11) states that constant values of upper layer thickness stream westward from their initial positions. The rates of westward propagation of h, however, are strongly dependent on h. For example, (11) predicts a zero westward propagation rate if either $h = 0$ or $h = H$. In between these two limits, i.e., when the fluid is somewhere stratified, nonzero westward propagation rates are predicted. The maximum propagation speed occurs for $h = H/2$.

The mechanism responsible for the westward motion is essentially that discussed by Rhines (1977) in the context of quasi-geostrophy. Large-scale north–south flows on a beta plane are horizontally divergent. Fluid column heights are drawn up and down by meridional flow in a manner that shifts the pressure distribution to the west. The quasi-geostrophic version of the PGWE may be extracted from (7) by considering small deviations of the interface about a resting value, which leads to nondispersive waves. The variation of propagation inherent in $c(h)$ [see (9)] is amplitude dependent and can be understood by rewriting the PGWE using geostrophy and (5). After some algebra, the PGWE becomes

$$\frac{\partial h}{\partial t} - \frac{\beta v_1 h}{f} = 0 \tag{12}$$

where the "other" term has been ignored, which states that net fluid column stretching on the beta plane is proportional to local mass flux; the greater the upper layer mass flux, the greater the stretching effect. The mass flux, $v_1 h$, originating in the continuity equation, is the nonlinear quantity responsible for the unique character of the PGWE.

Using the Sverdrup balance $v_1 h$ can be partially evaluated and, for a given thermocline slope, is proportional to $h - h^2/H$. If $h = 0$ or H, the Sverdrup constraint in the absence of wind requires that there be no meridional upper layer mass transport. In between, for a given slope, the net upper layer mass transport must be nonzero and maximum when $h = H/2$. This operates through (12) to force different westward propagation rates for columns of unequal height.

a. Steepening and its consequences

The method of characteristics solution can be used to trace out the system evolution for a given initial condition. The example shown in Fig. 3 is appropriate to a warm blob of fluid, from which it is immediately apparent that amplitude-dependent propagation leads to steepening. This is evidenced by the crossing of the characteristics in Fig. 3, at which point the solution contains a front in the thermocline.

The conditions under which this catastrophic steepening will occur can be determined by asking when

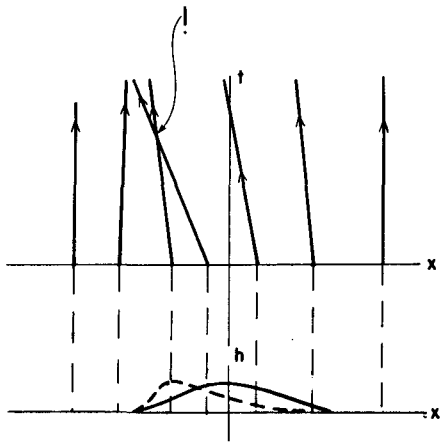

FIG. 3. Schematic of the characteristic solution. The rate of along-characteristic propagation depends on h, so arbitrary initial conditions lead to steepening. This appears in the phase plane as the drawing together of characteristics. The eventual intersection of two initially separated characteristics signals a breakdown of the solution.

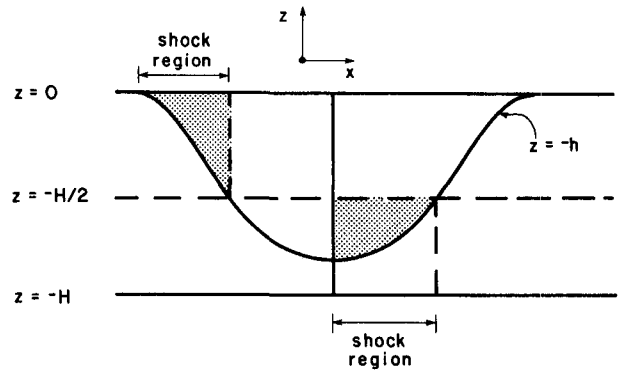

FIG. 4. Regions of shock formation. Shocks will form in the upper half of the fluid if the thermocline is thickening and in the lower half of the fluid if the thermocline is decreasing in thickness. The regions meeting the shock formation criteria for a thick warm blob of fluid are indicated by shading.

the zonal gradient of h will become large (i.e., when $h_x \to \infty$). Differentiating the implicit solution in (11) by x yields

$$h_x = \left[1 + \frac{\beta g'}{f^2}\left(h_x - \frac{2hh_x}{H}\right)t\right]h_0' \tag{13}$$

which may be solved for t to indicate when h_x becomes infinite:

$$t \approx f^2/[(\beta g'(1 - 2h/H))h_0'].$$

Here, h_0' denotes the first derivative of h_0. To be physically acceptable, the time t of shock formation must be positive. This is guaranteed from (13) if

$$(1 - 2h/H)h_0' > 0 \tag{14}$$

which characterizes regions in the initial condition where the thermocline is both getting thicker (thinner) toward the east and is shallower (deeper) than one half the total fluid depth. An initial condition corresponding to a warm blob of fluid is shown in Fig. 4. The regions where the constraints in (14) are met are indicated by the hatching.

The reasons why these regions lead to a catastrophic steepening of the initial condition are explained in Fig. 5. The Sverdrup constraint insures that the upper layer flow in Fig. 5a is to the north. According to (12), the thermocline must therefore be deepening. The absolute change in upper layer thickness is greatest at the point where $h = H/2$. The beta-induced tendency in the thermocline is thus as indicated by the dashed line in Fig. 5a, i.e., a considerably steepened thermocline in the region where $h < H/2$. Comparable arguments apply to Fig. 5b, except there the beta-induced tendency leads to a steeper profile for those parts of the thermocline deeper than $H/2$.

The nonlinearity responsible for this steepening tendency comes from the heat equations. A similar steepening tendency was noted by Anderson and Killworth (1979) and Johnson and Willmott (1981). Because their models implicitly assumed a resting deep ocean, they discovered the steepening tendency pertaining to the upper half of the fluid. The present model thus extends their results. The conditions that will lead to steepening are not very restrictive, suggesting frontogenesis by large-scale thermal anomalies is the rule rather than the exception and should be a general tendency in the ocean.

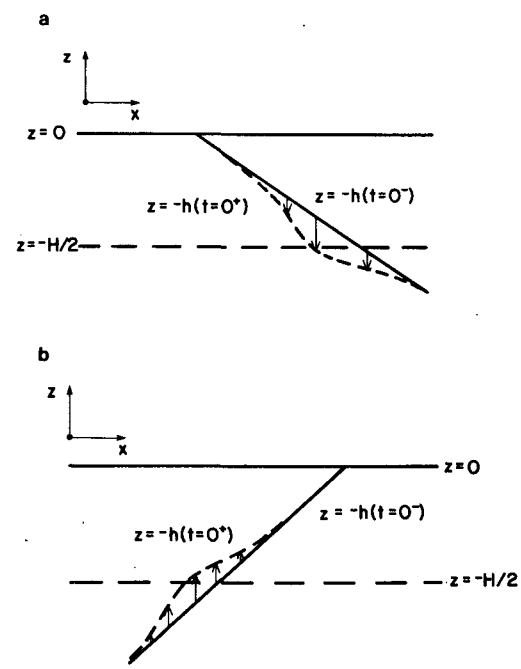

FIG. 5. Examples of steepening. Vortex tube stretching on a beta plane depends on net meridional mass transport. If $h_x > 0$, as in (a), upper layer mass transport is to the north and fluid columns must stretch to conserve potential vorticity. Because maximum stretching occurs when $h = H/2$, the tendency is for the thermocline to steepen in the upper half of the fluid. Similar arguments apply if $h_x < 0$, as in (b), and lead to steepening in the lower half of the fluid.

b. *Subplanetary-scale parameterizations*

As the thermocline steepens, effects in the "other" term [cf. (7)], which are generally small, must grow to finite amplitude and prevent the solution from becoming multivalued. Similar phenomena are noted in other prototype, nonlinear partial differential equations (e.g., Burgers' equation). The proper expression of the small scale and eddy effects is in itself an interesting problem; one way of determining their effects would be to begin a new scaling analysis, one which would, say, concentrate on the fronts. This approach is currently under study. For the remainder of this paper, however, the eddy effects will be expressed by including a diffusive term, Dh_{xx}, on the right-hand side of the PGWE, in place of the "other" term. This is undoubtedly the simplest possible parameterization of the effects of the smaller scales, but it is not altogether unreasonable. Diffusing heat down-gradient is equivalent to diffusing potential vorticity down-gradient. Rhines and Holland (1979) and Rhines and Young (1982a) argue that this is the effect of quasi-geostrophic eddies on the large-scale. Several general circulation models have since been based on this parameterization (Rhines and Young 1982b; Young and Rhines, 1982; Pedlosky and Young, 1983; DeSzoeke, 1985; Dewar, 1986; Cessi and Pedlosky, 1986), and eddy-resolving numerical models have supported it (Holland and Rhines, 1980). Also, the theory based on this parameterization is so simple that it merits a thorough examination prior to undertaking a more complicated analysis.

c. *Shock waves*

Upon employing heat diffusion on the right-hand side, the PGWE becomes

$$h_t+\frac{\beta g'}{f^2}\left(\frac{h^2h_x}{H}-hh_x\right)=Dh_{xx} \tag{15}$$

where the value of D is unspecified, but required to be small. Because the right-hand side of (15) is diffusive, as opposed to dispersive, the eventual balance obtained at the front is between steepening and dissipation (see Fig. 6). Such structures are referred to as "shock" waves because, in the limit of small D, property changes across the shocks can occur almost discontinuously.

Once formed, the shock behaves in a coherent manner and moves with a speed c_s that is calculable from (15). The value of c_s is found by first transforming (15) from the (x, t) frame, fixed in the fluid, to the frame defined by

$$x'=x-c_st$$

$$t'=t$$

which is fixed in the shock. Equation (15) in the shock frame is

$$h_{t'}-c_sh_{x'}+\frac{\beta g'}{f^2}\left(\frac{h^2}{H}h_{x'}-hh_{x'}\right)=Dh_{x'x'}. \tag{16}$$

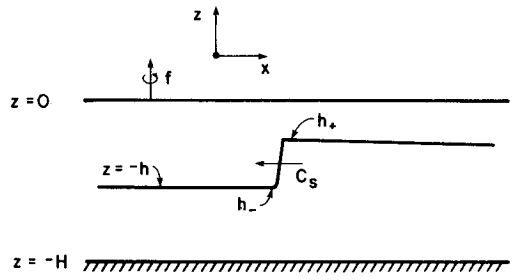

FIG. 6. Shock wave structure. Shock waves are coherent structures consisting of a balance between steepening and dissipation. The changes in fluid properties, in this case in h, can occur almost discontinuously. h_- refers to the thermocline thickness west of the shock, and h_+ refers to the thermocline thickness east of the shock. The shock propagation speed, c_s, can be computed from a knowledge of these parameters alone.

Integrating across the shock from $x'=-\epsilon$ to $x'=\epsilon$ (see Fig. 6), where ϵ is some location just outside the shock, and letting ϵ become small yields a formula for the shock speed c_s:

$$c_s=\frac{\beta g'}{f^2}\left(\frac{[h^3]}{3H}-\frac{[h^2]}{2}\right)\Big/[h]. \tag{17}$$

The square brackets denote the jump of the bracketed quantity across the shock:

$$[q]=q(\epsilon)-q(-\epsilon).$$

Introducing h_+ for the thermocline thickness east of the shock and h_- for the thermocline thickness west of the shock, (17) can be written as

$$c_s=\frac{\beta g'}{f^2}\left[\frac{h_+^2+h_+h_-+h_-^2}{3H}-\left(\frac{h_++h_-}{2}\right)\right]. \tag{18}$$

Note that c_s is independent of D.

d. *An initial value problem*

The next step is to use the partial solutions describing steepening, shock formation and propagation to solve an initial value problem. Consider the evolution of the initial state shown in Fig. 7. This corresponds to a cold plug of water sitting in an otherwise uniformly warm layer and is meant to crudely model a newly formed column of 18°C water. Given the state in Fig. 7, shock formation occurs instantly at both eastern and western edges of the column. Equation (18) demonstrates that shocks always propagate west, so the western shock will be named the "lead" shock, while the eastern shock will be called the "trail" shock.

The equations governing shock propagation are the shock maintenance conditions:

$$\dot{x}_s=c_s(h_+,h_-) \tag{19}$$

$$x_s(h_+,h_-)=x(h_+) \tag{20}$$

$$x_s(h_+,h_-)=x(h_-) \tag{21}$$

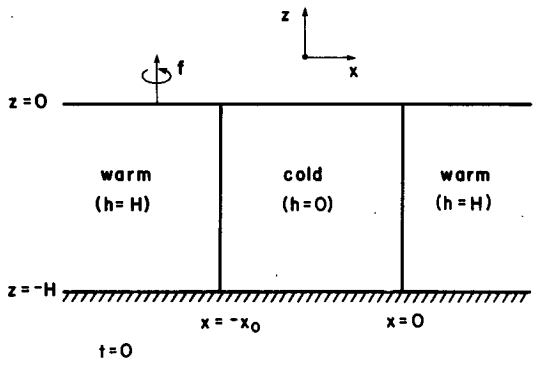

FIG. 7. Thermocline initial condition. The evolution of the above structure on a beta plane is computed using the planetary geostrophic wave equation augmented with weak diffusion. This initial condition was chosen as a crude model of a newly formed plug of 18°C water. Shock waves form from both edges of the initial condition. The western shock is called the "lead" shock and the eastern shock is called the "trail" shock.

where x_s denotes shock location, $x(h)$ denotes the location of fluid with thickness h, and the overdot denotes a time derivative. Equations (19)–(21) state that the shock propagates according to (18), and that it is both overrunning the structure ahead of it and being overrun by the structure behind it. First, for the lead shock, a little thought will convince the reader that h_- must be H. This is assured because $c(H) = 0$ [cf. (9)], so any nontrivial thermocline structure east of a point where $h = H$ must overrun that point. Solving (19) and (21) simultaneously then yields

$$h_+ = H/4.$$

Thus,

$$c_s = -\frac{3\beta g' H}{16 f^2}.$$

The parts of the western edge of the initial condition where $h < H/4$ move more slowly than the shock; their evolution can be computed by a characteristic solution that is modified to allow for the discontinuity in the initial thermocline structure. The solution for $h < H/4$ proceeds by defining a similarity variable:

$$\xi = x/t$$

and arguing that the characteristics depend only ξ (Whitham, 1974):

$$h = h_0(\xi). \tag{22}$$

Equation (7) can be converted to

$$[h_0'] \left[x + \frac{\beta g'}{f^2} h_0 t - \frac{\beta g'}{f^2} \frac{h_0^2 t}{H} \right] = 0 \tag{23}$$

from which the structure function for $h < H/4$ can be obtained:

$$h_0 = \frac{H}{2} - \frac{H}{2}\left(1 + \frac{4f^2}{\beta g' H}\frac{x}{t}\right)^{1/2}. \tag{24}$$

The other solution of the quadratic equation in (23) has been discarded so that (24) applies to the upper half of the fluid column. The similarity characteristics defined by (24) take the form of an expansion fan (see Fig. 13) and can be used to plot the thermocline structure for $h < H/4$ for any given time t.

A similar analysis applies to the trail edge of the initial condition, with the results that

$$h_- = 0$$

$$h_+ = 3H/4$$

$$c_s = \frac{-3\beta g' H}{16 f^2}.$$

An expansion fan defined by

$$h_0\left(\frac{x}{t}\right) = \frac{1}{2}H + \frac{1}{2}H\left(1 + \frac{4f^2}{\beta g' H}\frac{x}{t}\right)^{1/2}$$

applies where $3H/4 < h < H$. The trail shock structure is simply inverted from that of the lead shock. Both shocks propagate westward at the same rate.

The structure of this part of the solution is shown in Fig. 8, from which it is clear that the solution can hold only up to the time:

$$t_1 = \frac{16 x_0 f^2}{3 g' H \beta}.$$

After this, the trail shock will overtake the remnants of the lead initial condition, and a different solution must apply. This first part of the solution, which applies until time t_1, is referred to as double shock propagation.

e. *Shock overrun*

After t_1, the trail shock meets the remnants of the initial western column edge, and the system moves into a new phase of the solution, which is called the shock

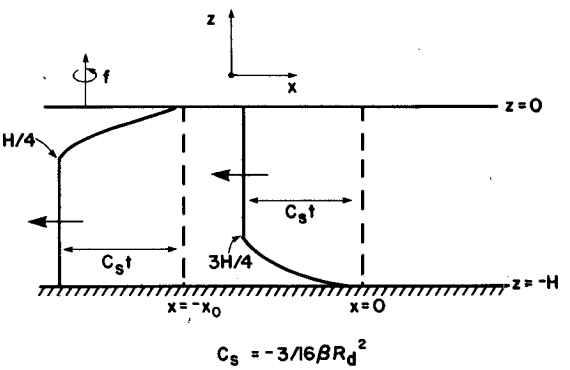

FIG. 8. Thermocline structure during double shock propagation. The lead and trail shocks propagate westward at the same speed, and both are $3H/4$ thick. The remainder of the solution consists of two expansion fans, emanating from the locations of the initial column condition edges.

overrun phase. The shock overrun solution consists of two relatively uninteresting parts and a third, more tantalizing part. First, the lead shock, unaware of any new events, continues westward as computed in the double shock propagation solution. Second, the characteristic solutions apply to the regions away from the shocks. Third, however, is the trail shock region, where qualitatively new phenomena appear.

The three parameters necessary to describe the trail shock evolution are h_+, h_- and x_s. These are governed by

$$c(h_+) = c_s(h_+, h_-) \tag{25}$$

$$c(h_-)t + x_0 = c(h_-)t - h_-/\alpha = x_s(h_+, h_-) \tag{26}$$

$$\dot{x}_s = c_s(h_+, h_-) \tag{27}$$

with the initial conditions $x_s = 0$, $h_+ = 3H/4$ and $h_- = 0$ at $t = 0$. Although the thermocline structure for $x < 0$ is known, it is not possible to write down closed form solutions to the system (25)–(27) if it is used. Analytical progress is possible, however, if a linear thermocline profile is used. This choice is reflected in (26), where α is the slope of the thermocline for $x < 0$ (see Fig. 9). Equations (25) and (26) are the shock maintenance conditions, while (27) is the shock propagation equation. Equation (25) can be solved for h_+ to yield

$$h_+ = \left(\frac{3H}{4} - \frac{h_-}{2}\right) \tag{28}$$

where the positive root of the quadratic has been discarded to meet the initial conditions. Substituting (28) in (27) and differentiating (26) yields an equation in h_-:

$$\frac{-\beta g'}{f^2}\left[\dot{h}_- - \frac{2\dot{h}_- h_-}{H}\right]t - \frac{\dot{h}_-}{\alpha} = \frac{\beta g'}{f^2}\left[\frac{3h_-}{4} - \frac{3h_-^2}{4H} - \frac{3H}{16}\right]. \tag{29}$$

The above equation, although nonlinear and nonconstant coefficient, can be solved by introducing a "warped" time variable, w, upon which time t depends:

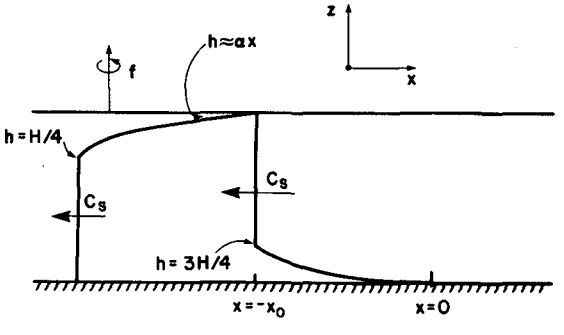

FIG. 9. Shock overrun initial structure. The double shock propagation solution breaks down when the trail shock encounters the remnants of the western initial condition. The evolution in this shock overrun phase is computed using the above initial condition, in which the reference frame has been centered on the shock and the thermocline structure west of the shock is assumed to increase linearly.

$$t = t(w),$$

along with the condition that $w = 0$ when $t = 0$.

This yields the coupled equations:

$$\frac{dt}{dw} = \left[\frac{-\beta g'}{f^2}\left(1 - \frac{2h_-}{H}\right)t - \frac{1}{\alpha}\right] \tag{30}$$

$$\frac{dh_-}{dw} = \frac{\beta g'}{f^2}\left[\frac{3h_-}{4} - \frac{3h_-^2}{4H} - \frac{3H}{16}\right]. \tag{31}$$

Equation (31) can be solved for h_- as a function of w. After eliminating h_- from (30), t can be solved in terms of w. Finally, these solutions can be joined to yield

$$t = \frac{-1}{\alpha}\frac{8f^2}{5\beta g'}\left(1 - \frac{2h_-}{H}\right)^{-1} + \frac{8f^2}{5\alpha\beta g'}\left(1 - \frac{2h_-}{H}\right)^{-8/3} \tag{32}$$

expressing t as a function of h_-.

One can, in principle, invert (32) for h_- as a function of t and then solve for h_+ using (28), and finally, for x_s using (26). On the other hand, the interesting features of the solution can be obtained from an asymptotic analysis of (32). For example, when $t = 0$, $h_- = 0$. Thus, for small t, $h_-/H \ll 1$, and

$$h_- = \frac{3\beta g' H\alpha t}{16 f^2} \tag{33}$$

or, for a short time the shock "slides" down the thermocline at the initial shock speed. The other result of interest is that as t becomes large, h_- tends asymptotically to $H/2$. From (28), h_+ must therefore also tend to $H/2$, indicating a gradual thinning of the shock (see Fig. 10).

The trail shock evolving in the presence of a linear thermocline tends to dissipate itself. Of course, in the present problem, this is not truly possible. Prior to achieving a value of $H/2$, h_- will obtain a value of $H/4$, and this corresponds to overrunning the lead shock. The trail shock is thus saved from total dissipation by an interaction with the lead shock. Note that this implies that the propagation speed of the trail shock increases. For example, if $h_- = H/4$, $h_+ = 5H/8$ and

$$c_s = \frac{-15}{64}\beta\frac{g'H}{f^2}$$

which is greater than the lead shock propagation speed of

$$c_s = \frac{-3}{16}\beta\frac{g'H}{f^2}.$$

The interaction of the trail and lead shocks marks the end of the shock overrun solution.

f. Shock joining

In the third phase of the solution, the two shocks join (see Fig. 11). It is clear from the asymptotic analysis of (32) that the trail shock accelerates in its propagation and, therefore, closes in on the lead shock. Interaction between the two shocks will necessarily occur when h_-

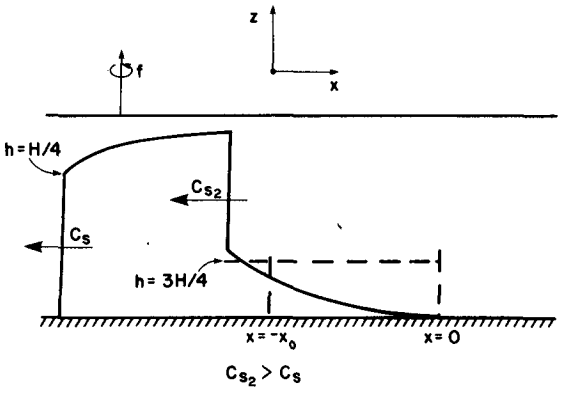

FIG. 10. Shock overrun solution. The trail shock decreases in thickness as it interacts with the western initial condition remnants. Both h_+ and h_- change in this process, and the trail shock picks up speed. The lead shock continues unchanged from its previous structure. The boundaries of the initial cold anomaly are labeled $-x_0$ and 0.

of the trail shock obtains the value $H/4$. According to (28), h_+ then obtains the value $5H/8$. In this problem, valid in the limit of weak diffusion, the interaction of the shocks is relatively simple. The volume of fluid between the shocks, i.e., the fluid with thickness values between $H/4$ and $5H/8$, monotonically decreases to zero, at which point the two shocks merge into one. The propagation of the lead shock changes discontinuously from the value it had prior to merger to the propagation speed of the merged shock. The merged shock is $3H/8$ thick and joined to the bottom. These points can be demonstrated by writing the PGWE in the frame of the lead shock prior to merger and noting that for vanishing diffusion the lead shock propagation rate remains constant until the trail shock contacts it. Of course, in a fluid with finite heat diffusion, the interaction of the shocks will be somewhat more complicated. I am currently studying this problem numerically; preliminary results show that the results listed above are a reasonable approximation to the solution with finite diffusion.

g. *Shock aging and death*

The final phase of evolution consists of shock aging and death, with the interesting part of the solution involving the propagation of the merged shock. Again the system can be solved if the thermocline structure is approximated by a linear function (see Fig. 12). The constraints on the shock are

$$h_- = H \tag{34}$$

$$x_s = \frac{5H}{8\alpha} - \frac{h_+}{\alpha} - \frac{\beta g'}{f^2}\left(h_+ - \frac{h_+^2}{H}\right)t \tag{35}$$

$$\dot{x}_s = c_s(h_+, h_-). \tag{36}$$

Equations (34) and (35) are the shock maintenance conditions and α is the slope of the thermocline for $x > 0$. Substituting (34) into (36) eliminates h_-, and x_s can be eliminated by differentiating (35) with respect to time. The final equation governing the shock is thus

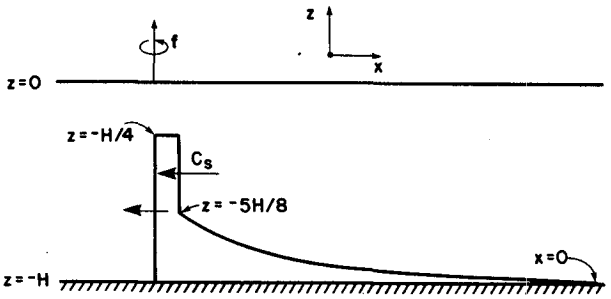

FIG. 11. Shock joining. The lead shock is eventually overrun by the trail shock. According to the asymptotics of the solution, the merged shock will be $3H/8$ thick and will be joined to the bottom. The eastern boundary of the initial cold anomaly is labeled $x = 0$.

$$\dot{h}_+\left(\frac{2\beta g' t h_+}{f^2 H} - \frac{\beta g' t}{f^2} - \frac{1}{\alpha}\right) = \frac{\beta g'}{f^2}\left(\frac{5h_+}{6} - \frac{2h_+^2}{3H} - \frac{H}{6}\right) \tag{37}$$

which can be solved in the same manner as (29). Introducing the warped time w, the coupled equations become

$$\frac{dt}{dw} = \frac{2\beta g' t h_+}{f^2 H} - \frac{\beta g' t}{f^2} - \frac{1}{\alpha} \tag{38}$$

$$\frac{dh_+}{dw} = \frac{-\beta g'}{6f^2}\frac{4}{H}(h_+ - H)\left(h_+ - \frac{H}{4}\right). \tag{39}$$

The solution to (39) yields one relation between h_+ and w:

$$\frac{h_+}{H} = \frac{\left(1 + \frac{1}{4}e^{-\beta g' w/(2f^2)}\right)}{(1 + e^{-\beta g' w/(2f^2)})}. \tag{40}$$

The h_+ can then be eliminated from (38), yielding a relation between t and w:

$$\frac{-\alpha\beta g'}{f^2}t = (1 + e^{-(\beta g' w/2f^2)})(e^{\beta g' w/f^2})(1 + 2e^{-\beta g' w/(2f^2)}) - \frac{3}{4}e^{\beta g' w/f^2}(1 + e^{-\beta g' w/(2f^2)})^3. \tag{41}$$

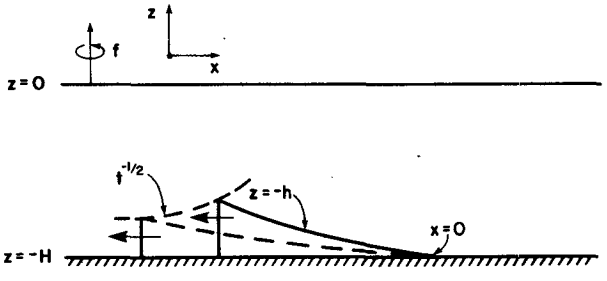

FIG. 12. Shock aging and death. In this final phase of the solution, the merged shock continues westward and experiences a slow $t^{-1/2}$ decay. The tendencies of the solution in this phase were computed by assuming a linear increase in h eastward from the point of the shock. The slope in h was taken to be α. The eastern boundary of the initial cold anomaly is labeled $x = 0$.

It is not generally possible to join (40) and (41) into one equation relating h_+ and t, but the asymptotic limits relating t and h_+ at small and large times can be obtained.

For small t it can be demonstrated that

$$t = -w/\alpha,$$

and that

$$\frac{h_+}{H} = \frac{5}{8} - \frac{3}{32}\frac{\beta g' \alpha t}{f^2}. \tag{42}$$

Equation (42) arises because cold fluid columns behind the shock are propagating initially at a rate of

$$c = \frac{-15}{64}\frac{\beta g' H}{f^2}$$

while the shock is moving at a rate of

$$c_s = \frac{-9}{64}\frac{\beta g' H}{f^2}.$$

The speed of the shock relative to that of the following fluid is

$$c - c_s = \frac{-3}{32}\frac{\beta g' H}{f^2}.$$

So, initially, the shock appears to slide backward down the thermocline slope and decrease in thickness.

For large t, the asymptotic limit is

$$\frac{-\alpha\beta g'}{f^2} t \sim \frac{1}{4} e^{\beta g' w / f^2},$$

and therefore,

$$\frac{h_+}{H} \sim 1 - \frac{3}{8}\left(\frac{|\alpha| g' \beta}{f^2}\right)^{-1/2} t^{-1/2}.$$

The shock, as it propagates west, decays slowly in amplitude and spreads the cold water over the bottom until there is no measurable lower layer thickness. At this point, the shock is "dead," $h = H$ everywhere, and no further evolution occurs.

The phase-plane solution for this problem is plotted in Fig. 13. The lighter lines emanating upward and westward from the x-axis are the regular characteristics. The two bold lines that merge to one bold line represent the movement of the shocks. The lighter horizontal lines, labeled t_1 and t_2, delineate the four phases of the solution. Figures 7 and 8 correspond to the solution from time 0 to time t_1, Figs. 9 and 10 to the time from t_1 to t_2, Fig. 11 to time t_2, and Fig. 12 to the times after t_2.

4. Discussion

The evolution of large-scale thermal anomalies has been computed. The equation governing their evolution (6) contains advection by the Sverdrup flow, westward beta-driven propagation, vortex stretching and buoyant forcing. A simplified version of this equation, valid in the absence of wind forcing, was considered. Buoyant forcing, while not explicitly included in the calculation, was implicit in the choice of initial condition. The system is thus governed by the PGWE, a first-order, nonlinear partial differential equation. Initial conditions evolving according to the PGWE steepen catastrophically. Under the assumption that the effects of the small scales can be parameterized as a heat diffusion, the steepening regions form shock waves and propagate with speeds dependent upon the shock structure.

The physical phenomenon motivating this work is the formation of 18°C water which, as observations suggest, occurs in an almost burstlike fashion. The evolution of a plug of cold water in an otherwise warm layer was considered. This initial condition was chosen as a crude model of newly formed 18°C water. Shocks formed at the eastern and western edges of the column. The subsequent evolution of the system divides neatly into four regimes, divided in character by the propagation of the shocks. In the first phase (double shock propagation), both shocks propagate uniformly to the west. This ends when the trail shock overtakes the remnants of western edge of the initial condition, and it is replaced by the shock overrun phase. During this phase, the trail shock gains speed and catches the lead shock. The next shock joining phase describes the merger of the two shocks into one and is followed by a gradual shock aging and death phase.

Two interesting aspects of the shock overrun solution are the acceleration of the trail shock and its attendant restructuring. These can be understood by recalling that the formula for shock propagation involves the variation in the thermocline thickness across the shock. In some sense, the shock waves propagate at a rate that is an average of all the propagation tendencies within the shock. These tendencies are weakest where the thermocline surfaces or meets the ocean bottom and increase in magnitude to a maximum when the thermocline is at a depth of half the fluid thickness. The trail shock, prior to the overrun phase, strikes the surface and is therefore slow in its propagation. As it overruns the western initial condition remnants, its western edge draws downward away from the surface. The shock, then composed of relatively faster propagation tendencies, picks up speed. Note that in the theoretical asymptotic limit the trail shock converges to $h_+ = h_- = H/2$ and disappears. This is because $h = H/2$ is a point of maximal propagation tendency.

a. Potential vorticity

The solutions presented here conserve net heat, in the sense that the quantity

$$I = \int_{-\infty}^{\infty} h dx$$

is independent of time. On the other hand, individual fluid columns conserve neither heat nor potential vor-

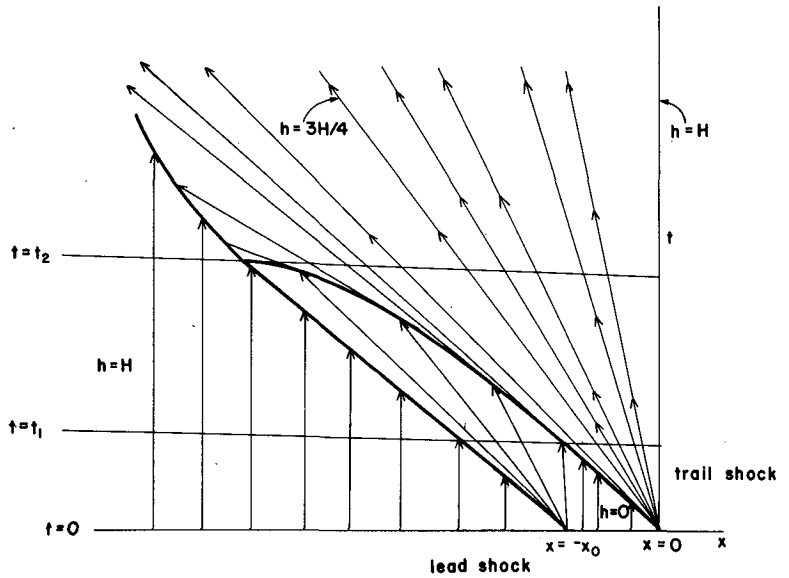

FIG. 13. Phase plane solution. The characteristics and paths of shock propagation in the x–t plane are plotted. The initial cold column was located between the point $x = 0$ and $x = -x_0$. The lighter lines are the regular characteristics and the darker lines are the shock characteristics. t_1 denotes the transition from double shock propagation to shock overrun, and t_2 the occurrence of shock joining. The shock aging and death solution applies for times greater than t_2.

ticity. The latter may be seen by rewriting (15) in terms of $q = f/h$:

$$q_t - \frac{\beta g'}{f^2}\left(f\frac{q_x}{q} - \frac{f^2}{H}\frac{q_x}{q^2}\right) = Dq_{xx} - \frac{2Dq_x^2}{q}.$$

It is a simple matter to show that most of the potential vorticity loss and heat diffusion in the fluid occurs in the shocks. Equation (15) is, of course, an approximate equation and describes only the large scale. Thus, the potential vorticity lost from the large scale should appear at smaller scales and involve relative vorticity. Shocks should therefore be sources of mesoscale variability.

It is also apparent that shock waves can transport heat and potential vorticity substantial distances from the buoyant source regions (e.g., compare Figs. 7 and 12). The suggestion, therefore, is that shock waves, should they exist in the ocean, might play a major role in determining the large-scale distributions of heat, potential vorticity and mesoscale energy. As such, they would have an important effect on climate and possibly be a mechanism for ventilating the thermocline.

Shock waves that arise in other fluid mechanics situations dissipate fairly rapidly, especially when compared to permanent wave soliton solutions, which consist of a balance between steepening and dispersive tendencies. There are two related points to be made here. First, a dispersivelike mechanism is available in this problem, i.e., relative vorticity generation. It might therefore be possible to generate permanent form solutions if this mechanism is included. The intent of this paper was to examine thermocline evolution as governed by a simpler system, although work on in-

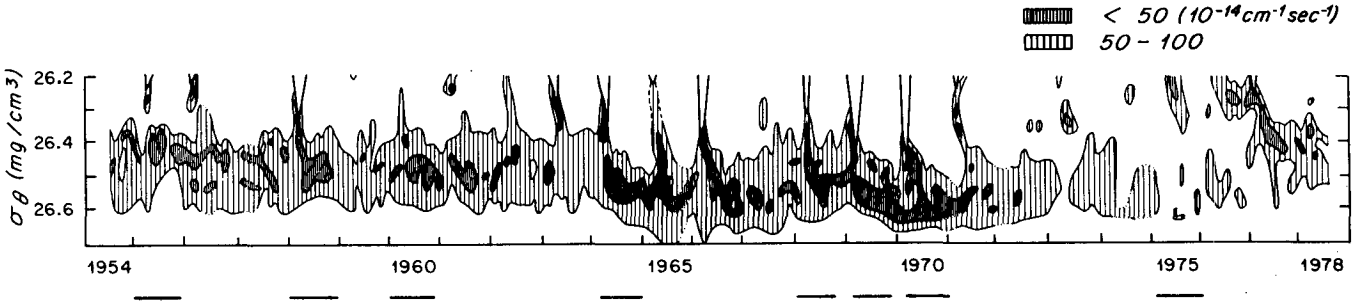

FIG. 14. A 24-year time series of potential vorticity at several depths from Panulirus. This figure appeared originally in Talley and Raymer (1982). Lowest potential vorticity values are shaded darkest. Minimum potential vorticity values correspond to the arrival of newly formed 18°C water.

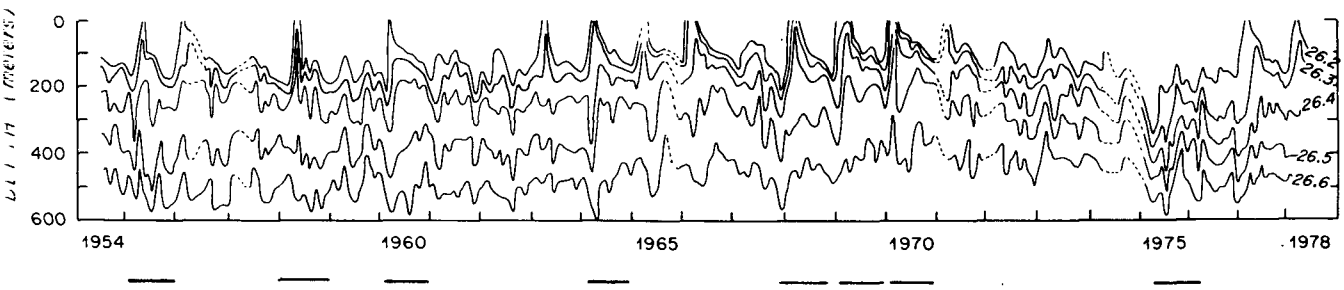

FIG. 15. A 24-year time series of density at several depths from Panulirus. This figure appeared originally in Talley and Raymer (1982). The σ_θ 26.5 surface is associated with 18°C water. Newly formed 18°C water, defined by minimum potential vorticity values (see Fig. 14), arrives in sharp, [illegible] events. Several are indicated by underlining. The analysis suggests beta-driven steepening as a mechanism for maintaining these fronts.

cluding relative vorticity is currently under way. Whereas relative vorticity generation balancing steepening might occur when the front is stable, the present work might be thought to apply to a front that is unstable and therefore generating deformation-scale geostrophic turbulence. Second, it is worth mentioning that the double shock propagation tendency of this system tends to make planetary shocks a long-lived phenomenon. This is because the lead and trail shocks move at the same rate, and the usual mechanism of shock decay (i.e., faster-moving structure behind the shock overrunning the shock) is considerably reduced in efficiency. Planetary shocks can thus be expected to be long-lived.

b. Data

With respect to observations, there are apparently no data that can conclusively address the existence of planetary shocks, not a surprising result given the necessity of locating and following the evolution of a newly formed plug of 18°C water. There are, however, some suggestive data. Figures 14 and 15, reproductions of figures that originally appeared in Talley and Raymer (1982), contain 24 years worth of density and potential vorticity data from the Panulirus station near Bermuda. It is commonly thought that this station is located within the wind-driven circulation and on the edge of the inertial recirculation. Accordingly, the data are dominated by events which, as convincingly argued by Talley and Raymer (1982), are of the proper phasing, potential vorticity and density to be asociated with the upstream formation of 18°C water. The defining characteristic of newly formed 18°C water is the occurrence of a minimum in potential vorticity with a potential density of $\sigma_\theta = 26.5$. What the eye picks out in Fig. 15 is the arrival of several very abrupt variations in the depth of the $\sigma_\theta = 26.5$ surface. Minima in potential vorticity are associated with these events, suggesting this is a standard form for new 18°C water to obtain. While the data are far from conclusive, it is certainly tempting to argue that these fronts are not inconsistent with the present model. Talley and Raymer (1982) argue that these abrupt events are dominated by their convective origins and subsequent advection by the large-scale. To these, I would like to add two other effects. First, this analysis shows that an 18°C plug should be somewhat self-propelling. Self-propagation speeds for these plugs are O(1) cm s^{-1}, which is comparable to advection by the Sverdrup transport, so both effects should be of equal importance in the movement of 18°C water. Second, the sharp structure of these events in the Panulirus data might be partly due to the tendency for finite amplitude thermal anomalies to steepen. This mechanism could, for example, maintain the convectively generated fronts as they move from their generation point to Panulirus.

Acknowledgments. It is a pleasure to recognize the interest and input of Drs. John M. Bane and Peter B. Rhines to this work. An anonymous reviewer is also thanked for a careful reading of this paper and for many constructive criticisms. Figures 14 and 15 appeared originally in a paper by Talley and Raymer (1982) and appear here by their kind permission. My research is sponsored by NSF Grant OCE 8415475 to the University of North Carolina. Pat Klein, who typed the manuscript, is thanked for her good humor and patience.

REFERENCES

Anderson, D., and A. Gill, 1975: Spin-up of a stratified ocean with applications to upwelling. *Deep-Sea Res.*, **22**, 583–596.

——, and P. Killworth, 1977: Spin-up of a stratified ocean, with topography. *Deep-Sea Res.*, **24**, 709–732.

——, and ——, 1979: Non-linear propagation of long Rossby waves. *Deep-Sea Res.*, **26**, 1033–1050.

Cessi, P., and J. Pedlosky, 1986: On the role of topography in the ocean circulation. *J. Mar. Res.*, **44**, 445–471.

Cushman-Roisin, B., 1987: On the role of heat flux in the Gulf Stream, Sargusso Sea, subtropical gyre system. *J. Phys. Oceanogr.* (in press)

deSzoeke, R., 1985: Wind-driven mid-ocean baroclinic gyres over topography: A circulation equation extending the Sverdrup relation. *J. Mar. Res.*, **43**, 793–824.

Dewar, W., 1986: On the potential vorticity structure of weakly ventilated isopycnals: A theory of subtropical mode water maintenance. *J. Phys. Oceanogr.*, **16**, 1204–1216.

——, P. Rhines and W. Young, 1984: The nonlinear spin-up of a stratified ocean. *Geophys. Astrophys. Fluid Dyn.*, **30**, 169–197.

Holland, W., and P. Rhines, 1980: An example of eddy-induced ocean circulation. *J. Phys. Oceanogr.*, **10,** 1010–1031.

Johnson, J., and A. Willmott, 1981: An unsteady wind-driven ocean circulation model. *Dyn. Atmos. Ocean,* **6,** 1–27.

Keffer, T., 1985: The ventilation of the world's oceans: Maps of the potential vorticity field. *J. Phys. Oceanogr.*, **15,** 509–523.

Luyten, J., J. Pedlosky and H. Stommel, 1983: The ventilated thermocline. *J. Phys. Oceanogr.*, **13,** 292–309.

McDowell, S., P. Rhines and T. Keffer, 1982: North Atlantic potential vorticity and its relation to the general circulation. *J. Phys. Oceanogr.*, **12,** 1417–1436.

Pedlosky, J., 1979: *Geophysical Fluid Dynamics.* Springer-Verlag, 624 pp.

——, and W. Young, 1983: Ventilation, potential-vorticity homogenization and the structure of the ocean circulation. *J. Phys. Oceanogr.*, **13,** 2020–2037.

Rhines, P., 1977: The dynamics of unsteady currents. *The Sea,* Vol. 6, E. D. Goldberg, I. N. McCabe, J. J. O'Brien and J. H. Steele, Eds., Wiley, 189–318.

——, and W. Holland, 1979: A theoretical discussion of eddy-driven mean flows. *Dyn. Atmos. Oceans,* **3,** 289–325.

——, and W. Young, 1982a: Homogenization of potential vorticity in planetary gyres. *J. Fluid Mech.*, **122,** 347–367.

——, and ——, 1982b: A theory of the wind-driven circulation, I. Mid-ocean gyres. *J. Mar. Res.*, **40**(Suppl), 559–596.

Talley, L., and M. Raymer, 1982: Eighteen degree water variability. *J. Mar. Res.*, **40**(Suppl.), 757–775.

Whitman, G., 1974: *Linear and Nonlinear Waves.* Wiley-Interscience, 636 pp.

Willmott, A., 1985: A note on the steepening of long Rossby waves. *Deep-Sea Res.*, **32,** 613–617.

Young, W., and P. Rhines, 1982: A theory of the wind-driven circulation, II. Gyres with western boundary layers. *J. Mar. Res.*, **40,** 849–872.